

Search for $B_s^0 \rightarrow \mu^+ \mu^-$ and $B^0 \rightarrow \mu^+ \mu^-$ Decays with 2 fb^{-1} of $p\bar{p}$ Collisions

T. Aaltonen,²³ J. Adelman,¹³ T. Akimoto,⁵⁴ M. G. Albrow,¹⁷ B. Álvarez González,¹¹ S. Amerio,⁴² D. Amidei,³⁴ A. Anastassov,⁵¹ A. Annovi,¹⁹ J. Antos,¹⁴ M. Aoki,²⁴ G. Apollinari,¹⁷ A. Apresyan,⁴⁷ T. Arisawa,⁵⁶ A. Artikov,¹⁵ W. Ashmanskas,¹⁷ A. Attal,³ A. Aurisano,⁵² F. Azfar,⁴¹ P. Azzi-Bacchetta,⁴² P. Azzurri,⁴⁵ N. Bacchetta,⁴² W. Badgett,¹⁷ A. Barbaro-Galtieri,²⁸ V. E. Barnes,⁴⁷ B. A. Barnett,²⁵ S. Baroiant,⁷ V. Bartsch,³⁰ G. Bauer,³² P.-H. Beauchemin,³³ F. Bedeschi,⁴⁵ P. Bednar,¹⁴ S. Behari,²⁵ G. Bellettini,⁴⁵ J. Bellinger,⁵⁸ A. Belloni,²² D. Benjamin,¹⁶ A. Beretvas,¹⁷ J. Beringer,²⁸ T. Berry,²⁹ A. Bhatti,⁴⁹ M. Binkley,¹⁷ D. Bisello,⁴² I. Bizjak,³⁰ R. E. Blair,² C. Blocker,⁶ B. Blumenfeld,²⁵ A. Bocci,¹⁶ A. Bodek,⁴⁸ V. Boisvert,⁴⁸ G. Bolla,⁴⁷ A. Bolshov,³² D. Bortoletto,⁴⁷ J. Boudreau,⁴⁶ A. Boveia,¹⁰ B. Brau,¹⁰ A. Bridgeman,²⁴ L. Brigliadori,⁵ C. Bromberg,³⁵ E. Brubaker,¹³ J. Budagov,¹⁵ H. S. Budd,⁴⁸ S. Budd,²⁴ K. Burkett,¹⁷ G. Busetto,⁴² P. Bussey,²¹ A. Buzatu,³³ K. L. Byrum,² S. Cabrera,^{16,r} M. Campanelli,³⁵ M. Campbell,³⁴ F. Canelli,¹⁷ A. Canepa,⁴⁴ D. Carlsmith,⁵⁸ R. Carosi,⁴⁵ S. Carrillo,^{18,l} S. Carron,³³ B. Casal,¹¹ M. Casarsa,¹⁷ A. Castro,⁵ P. Catastini,⁴⁵ D. Cauz,⁵³ M. Cavalli-Sforza,³ A. Cerri,²⁸ L. Cerrito,^{30,p} S. H. Chang,²⁷ Y. C. Chen,¹ M. Chertok,⁷ G. Chiarelli,⁴⁵ G. Chlachidze,¹⁷ F. Chlebana,¹⁷ K. Cho,²⁷ D. Chokheli,¹⁵ J. P. Chou,²² G. Choudalakis,³² S. H. Chuang,⁵¹ K. Chung,¹² W. H. Chung,⁵⁸ Y. S. Chung,⁴⁸ C. I. Ciobanu,²⁴ M. A. Ciocci,⁴⁵ A. Clark,²⁰ D. Clark,⁶ G. Compostella,⁴² M. E. Convery,¹⁷ J. Conway,⁷ B. Cooper,³⁰ K. Copic,³⁴ M. Cordelli,¹⁹ G. Cortiana,⁴² F. Crescioli,⁴⁵ C. Cuenca Almenar,^{7,r} J. Cuevas,^{11,o} R. Culbertson,¹⁷ J. C. Cully,³⁴ D. Dagenhart,¹⁷ M. Datta,¹⁷ T. Davies,²¹ P. de Barbaro,⁴⁸ S. De Cecco,⁵⁰ A. Deisher,²⁸ G. De Lentdecker,^{48,d} G. De Lorenzo,³ M. Dell'Orso,⁴⁵ L. Demortier,⁴⁹ J. Deng,¹⁶ M. Deninno,⁵ D. De Pedis,⁵⁰ P. F. Derwent,¹⁷ G. P. Di Giovanni,⁴³ C. Dionisi,⁵⁰ B. Di Ruzza,⁵³ J. R. Dittmann,⁴ M. D'Onofrio,³ S. Donati,⁴⁵ P. Dong,⁸ J. Donini,⁴² T. Dorigo,⁴² S. Dube,⁵¹ J. Efron,³⁸ R. Erbacher,⁷ D. Errede,²⁴ S. Errede,²⁴ R. Eusebi,¹⁷ H. C. Fang,²⁸ S. Farrington,²⁹ W. T. Fedorko,¹³ R. G. Feild,⁵⁹ M. Feindt,²⁶ J. P. Fernandez,³¹ C. Ferrazza,⁴⁵ R. Field,¹⁸ G. Flanagan,⁴⁷ R. Forrest,⁷ S. Forrester,⁷ M. Franklin,²² J. C. Freeman,²⁸ I. Furic,¹⁸ M. Gallinaro,⁴⁹ J. Galyardt,¹² F. Garbersson,¹⁰ J. E. Garcia,⁴⁵ A. F. Garfinkel,⁴⁷ K. Genser,¹⁷ H. Gerberich,²⁴ D. Gerdes,³⁴ S. Giagu,⁵⁰ V. Giakoumopolou,^{45,a} P. Giannetti,⁴⁵ K. Gibson,⁴⁶ J. L. Gimmell,⁴⁸ C. M. Ginsburg,¹⁷ N. Giokaris,^{15,a} M. Giordani,⁵³ P. Giromini,¹⁹ M. Giunta,⁴⁵ V. Glagolev,¹⁵ D. Glenzinski,¹⁷ M. Gold,³⁶ N. Goldschmidt,¹⁸ A. Golossanov,¹⁷ G. Gomez,¹¹ G. Gomez-Ceballos,³² M. Goncharov,⁵² O. González,³¹ I. Gorelov,³⁶ A. T. Goshaw,¹⁶ K. Goulianos,⁴⁹ A. Gresele,⁴² S. Grinstein,²² C. Grosso-Pilcher,¹³ R. C. Group,¹⁷ U. Grundler,²⁴ J. Guimaraes da Costa,²² Z. Gunay-Unalan,³⁵ C. Haber,²⁸ K. Hahn,³² S. R. Hahn,¹⁷ E. Halkiadakis,⁵¹ A. Hamilton,²⁰ B.-Y. Han,⁴⁸ J. Y. Han,⁴⁸ R. Handler,⁵⁸ F. Happacher,¹⁹ K. Hara,⁵⁴ D. Hare,⁵¹ M. Hare,⁵⁵ S. Harper,⁴¹ R. F. Harr,⁵⁷ R. M. Harris,¹⁷ M. Hartz,⁴⁶ K. Hatakeyama,⁴⁹ J. Hauser,⁸ C. Hays,⁴¹ M. Heck,²⁶ A. Heijboer,⁴⁴ B. Heinemann,²⁸ J. Heinrich,⁴⁴ C. Henderson,³² M. Herndon,⁵⁸ J. Heuser,²⁶ S. Hewamanage,⁴ D. Hidas,¹⁶ C. S. Hill,^{10,c} D. Hirschbuehl,²⁶ A. Hocker,¹⁷ S. Hou,¹ M. Houlden,²⁹ S.-C. Hsu,⁹ B. T. Huffman,⁴¹ R. E. Hughes,³⁸ U. Husemann,⁵⁹ J. Huston,³⁵ J. Incandela,¹⁰ G. Introzzi,⁴⁵ M. Iori,⁵⁰ A. Ivanov,⁷ B. Iyutin,³² E. James,¹⁷ B. Jayatilaka,¹⁶ D. Jeans,⁵⁰ E. J. Jeon,²⁷ S. Jindariani,¹⁸ W. Johnson,⁷ M. Jones,⁴⁷ K. K. Joo,²⁷ S. Y. Jun,¹² J. E. Jung,²⁷ T. R. Junk,²⁴ T. Kamon,⁵² D. Kar,¹⁸ P. E. Karchin,⁵⁷ Y. Kato,⁴⁰ R. Kephart,¹⁷ U. Kerzel,²⁶ V. Khotilovich,⁵² B. Kilminster,³⁸ D. H. Kim,²⁷ H. S. Kim,²⁷ J. E. Kim,²⁷ M. J. Kim,¹⁷ S. B. Kim,²⁷ S. H. Kim,⁵⁴ Y. K. Kim,¹³ N. Kimura,⁵⁴ L. Kirsch,⁶ S. Klimenko,¹⁸ M. Klute,³² B. Knuteson,³² B. R. Ko,¹⁶ S. A. Koay,¹⁰ K. Kondo,⁵⁶ D. J. Kong,²⁷ J. Konigsberg,¹⁸ A. Korytov,¹⁸ A. V. Kotwal,¹⁶ J. Kraus,²⁴ M. Kreps,²⁶ J. Kroll,⁴⁴ N. Krumnack,⁴ M. Kruse,¹⁶ V. Krutelyov,¹⁰ T. Kubo,⁵⁴ S. E. Kuhlmann,² T. Kuhr,²⁶ N. P. Kulkarni,⁵⁷ Y. Kusakabe,⁵⁶ S. Kwang,¹³ A. T. Laasanen,⁴⁷ S. Lai,³³ S. Lami,⁴⁵ S. Lammel,¹⁷ M. Lancaster,³⁰ R. L. Lander,⁷ K. Lannon,³⁸ A. Lath,⁵¹ G. Latino,⁴⁵ I. Lazzizzera,⁴² T. LeCompte,² J. Lee,⁴⁸ J. Lee,²⁷ Y. J. Lee,²⁷ S. W. Lee,^{52,q} R. Lefèvre,²⁰ N. Leonardo,³² S. Leone,⁴⁵ S. Levy,¹³ J. D. Lewis,¹⁷ C. Lin,⁵⁹ C. S. Lin,²⁸ J. Linacre,⁴¹ M. Lindgren,¹⁷ E. Lipeles,⁹ A. Lister,⁷ D. O. Litvintsev,¹⁷ T. Liu,¹⁷ N. S. Lockyer,⁴⁴ A. Loginov,⁵⁹ M. Loreti,⁴² L. Lovas,¹⁴ R.-S. Lu,¹ D. Lucchesi,⁴² J. Lueck,²⁶ C. Luci,⁵⁰ P. Lujan,²⁸ P. Lukens,¹⁷ G. Lungu,¹⁸ L. Lyons,⁴¹ J. Lys,²⁸ R. Lysak,¹⁴ E. Lytken,⁴⁷ P. Mack,²⁶ D. MacQueen,³³ R. Madrak,¹⁷ K. Maeshima,¹⁷ K. Makhoul,³² T. Maki,²³ P. Maksimovic,²⁵ S. Malde,⁴¹ S. Malik,³⁰ G. Manca,²⁹ A. Manousakis,^{15,a} F. Margaroli,⁴⁷ C. Marino,²⁶ C. P. Marino,²⁴ A. Martin,⁵⁹ M. Martin,²⁵ V. Martin,^{21,j} M. Martínez,³ R. Martínez-Ballarín,³¹ T. Maruyama,⁵⁴ P. Mastrandrea,⁵⁰ T. Masubuchi,⁵⁴ M. E. Mattson,⁵⁷ P. Mazzanti,⁵ K. S. McFarland,⁴⁸ P. McIntyre,⁵² R. McNulty,^{29,i} A. Mehta,²⁹ P. Mehtala,²³ S. Menzemer,^{11,k} A. Menzione,⁴⁵ P. Merkel,⁴⁷ C. Mesropian,⁴⁹ A. Messina,³⁵ T. Miao,¹⁷ N. Miladinovic,⁶ J. Miles,³² R. Miller,³⁵ C. Mills,²² M. Milnik,²⁶ A. Mitra,¹ G. Mitselmakher,¹⁸ H. Miyake,⁵⁴ S. Moed,²² N. Moggi,⁵ C. S. Moon,²⁷ R. Moore,¹⁷ M. Morello,⁴⁵ P. Movilla Fernandez,²⁸ J. Mülmenstädt,²⁸ A. Mukherjee,¹⁷ Th. Muller,²⁶ R. Mumford,²⁵ P. Murat,¹⁷ M. Mussini,⁵ J. Nachtman,¹⁷ Y. Nagai,⁵⁴ A. Nagano,⁵⁴ J. Naganoma,⁵⁶ K. Nakamura,⁵⁴

I. Nakano,³⁹ A. Napier,⁵⁵ V. Necula,¹⁶ C. Neu,⁴⁴ M. S. Neubauer,²⁴ J. Nielsen,^{28,f} L. Nodulman,² M. Norman,⁹ O. Norniella,²⁴ E. Nurse,³⁰ S. H. Oh,¹⁶ Y. D. Oh,²⁷ I. Oksuzian,¹⁸ T. Okusawa,⁴⁰ R. Oldeman,²⁹ R. Orava,²³ K. Osterberg,²³ S. Pagan Griso,⁴² C. Pagliarone,⁴⁵ E. Palencia,¹⁷ V. Papadimitriou,¹⁷ A. Papaikonomou,²⁶ A. A. Paramonov,¹³ B. Parks,³⁸ S. Pashapour,³³ J. Patrick,¹⁷ G. Pauletta,⁵³ M. Paulini,¹² C. Paus,³² D. E. Pellett,⁷ A. Penzo,⁵³ T. J. Phillips,¹⁶ G. Piacentino,⁴⁵ J. Piedra,⁴³ L. Pinares,¹⁸ K. Pitts,²⁴ C. Plager,⁸ L. Pondrom,⁵⁸ X. Portell,³ O. Poukhov,¹⁵ N. Pounder,⁴¹ F. Prakoshyn,¹⁵ A. Pronko,¹⁷ J. Proudfoot,² F. Ptohos,^{17,h} G. Punzi,⁴⁵ J. Pursley,⁵⁸ J. Rademacker,^{41,c} A. Rahaman,⁴⁶ V. Ramakrishnan,⁵⁸ N. Ranjan,⁴⁷ I. Redondo,³¹ B. Reisert,¹⁷ V. Rekovic,³⁶ P. Renton,⁴¹ M. Rescigno,⁵⁰ S. Richter,²⁶ F. Rimondi,⁵ L. Ristori,⁴⁵ A. Robson,²¹ T. Rodrigo,¹¹ E. Rogers,²⁴ S. Rolli,⁵⁵ R. Roser,¹⁷ M. Rossi,⁵³ R. Rossin,¹⁰ P. Roy,³³ A. Ruiz,¹¹ J. Russ,¹² V. Rusu,¹⁷ H. Saarikko,²³ A. Safonov,⁵² W. K. Sakumoto,⁴⁸ G. Salamanna,⁵⁰ O. Saltó,³ L. Santi,⁵³ S. Sarkar,⁵⁰ L. Sartori,⁴⁵ K. Sato,¹⁷ A. Savoy-Navarro,⁴³ T. Scheidle,²⁶ P. Schlabach,¹⁷ E. E. Schmidt,¹⁷ M. A. Schmidt,¹³ M. P. Schmidt,⁵⁹ M. Schmitt,³⁷ T. Schwarz,⁷ L. Scodellaro,¹¹ A. L. Scott,¹⁰ A. Scribano,⁴⁵ F. Scuri,⁴⁵ A. Sedov,⁴⁷ S. Seidel,³⁶ Y. Seiya,⁴⁰ A. Semenov,¹⁵ L. Sexton-Kennedy,¹⁷ A. Sfyria,²⁰ S. Z. Shalhout,⁵⁷ M. D. Shapiro,²⁸ T. Shears,²⁹ P. F. Shepard,⁴⁶ D. Sherman,²² M. Shimojima,^{54,n} M. Shochet,¹³ Y. Shon,⁵⁸ I. Shreyber,²⁰ A. Sidoti,⁴⁵ P. Sinervo,³³ A. Sisakyan,¹⁵ A. J. Slaughter,¹⁷ J. Slaunwhite,³⁸ K. Sliwa,⁵⁵ J. R. Smith,⁷ F. D. Snider,¹⁷ R. Snihur,³³ M. Soderberg,³⁴ A. Soha,⁷ S. Somalwar,⁵¹ V. Sorin,³⁵ J. Spalding,¹⁷ F. Spinella,⁴⁵ T. Spreitzer,³³ P. Squillacioti,⁴⁵ M. Stanitzki,⁵⁹ R. St. Denis,²¹ B. Stelzer,⁸ O. Stelzer-Chilton,⁴¹ D. Stentz,³⁷ J. Strologas,³⁶ D. Stuart,¹⁰ J. S. Suh,²⁷ A. Sukhanov,¹⁸ H. Sun,⁵⁵ I. Suslov,¹⁵ T. Suzuki,⁵⁴ A. Taffard,^{24,e} R. Takashima,³⁹ Y. Takeuchi,⁵⁴ R. Tanaka,³⁹ M. Tecchio,³⁴ P. K. Teng,¹ K. Terashi,⁴⁹ J. Thom,^{17,g} A. S. Thompson,²¹ G. A. Thompson,²⁴ E. Thomson,⁴⁴ P. Tipton,⁵⁹ V. Tiwari,¹² S. Tkaczyk,¹⁷ D. Toback,⁵² S. Tokar,¹⁴ K. Tollefson,³⁵ T. Tomura,⁵⁴ D. Tonelli,¹⁷ S. Torre,¹⁹ D. Torretta,¹⁷ S. Tourneur,⁴³ W. Trischuk,³³ Y. Tu,⁴⁴ N. Turini,⁴⁵ F. Ukegawa,⁵⁴ S. Uozumi,⁵⁴ S. Vallecorsa,²⁰ N. van Remortel,²³ A. Varganov,³⁴ E. Vataga,³⁶ F. Vázquez,^{18,l} G. Velev,¹⁷ C. Vellidis,^{45,a} V. Veszpremi,⁴⁷ M. Vidal,³¹ R. Vidal,¹⁷ I. Vila,¹¹ R. Vilar,¹¹ T. Vine,³⁰ M. Vogel,³⁶ I. Volobouev,^{28,q} G. Volpi,⁴⁵ F. Würthwein,⁹ P. Wagner,⁴⁴ R. G. Wagner,² R. L. Wagner,¹⁷ J. Wagner-Kuhr,²⁶ W. Wagner,²⁶ T. Wakisaka,⁴⁰ R. Wallny,⁸ S. M. Wang,¹ A. Warburton,³³ D. Waters,³⁰ M. Weinberger,⁵² W. C. Wester III,¹⁷ B. Whitehouse,⁵⁵ D. Whiteson,^{44,e} A. B. Wicklund,² E. Wicklund,¹⁷ G. Williams,³³ H. H. Williams,⁴⁴ P. Wilson,¹⁷ B. L. Winer,³⁸ P. Wittich,^{17,g} S. Wolbers,¹⁷ C. Wolfe,¹³ T. Wright,³⁴ X. Wu,²⁰ S. M. Wynne,²⁹ A. Yagil,⁹ K. Yamamoto,⁴⁰ J. Yamaoka,⁵¹ T. Yamashita,³⁹ C. Yang,⁵⁹ U. K. Yang,^{13,m} Y. C. Yang,²⁷ W. M. Yao,²⁸ G. P. Yeh,¹⁷ J. Yoh,¹⁷ K. Yorita,¹³ T. Yoshida,⁴⁰ G. B. Yu,⁴⁸ I. Yu,²⁷ S. S. Yu,¹⁷ J. C. Yun,¹⁷ L. Zanello,⁵⁰ A. Zanetti,⁵³ I. Zaw,²² X. Zhang,²⁴ Y. Zheng,^{8,b} and S. Zucchelli⁵

(CDF Collaboration)

¹*Institute of Physics, Academia Sinica, Taipei, Taiwan 11529, Republic of China*²*Argonne National Laboratory, Argonne, Illinois 60439, USA*³*Institut de Física d'Altes Energies, Universitat Autònoma de Barcelona, E-08193, Bellaterra (Barcelona), Spain*⁴*Baylor University, Waco, Texas 76798, USA*⁵*Istituto Nazionale di Fisica Nucleare, University of Bologna, I-40127 Bologna, Italy*⁶*Brandeis University, Waltham, Massachusetts 02254, USA*⁷*University of California, Davis, Davis, California 95616, USA*⁸*University of California, Los Angeles, Los Angeles, California 90024, USA*⁹*University of California, San Diego, La Jolla, California 92093, USA*¹⁰*University of California, Santa Barbara, Santa Barbara, California 93106, USA*¹¹*Instituto de Física de Cantabria, CSIC-University of Cantabria, 39005 Santander, Spain*¹²*Carnegie Mellon University, Pittsburgh, Pennsylvania 15213, USA*¹³*Enrico Fermi Institute, University of Chicago, Chicago, Illinois 60637, USA*¹⁴*Comenius University, 842 48 Bratislava, Slovakia; Institute of Experimental Physics, 040 01 Kosice, Slovakia*¹⁵*Joint Institute for Nuclear Research, RU-141980 Dubna, Russia*¹⁶*Duke University, Durham, North Carolina 27708*¹⁷*Fermi National Accelerator Laboratory, Batavia, Illinois 60510, USA*¹⁸*University of Florida, Gainesville, Florida 32611, USA*¹⁹*Laboratori Nazionali di Frascati, Istituto Nazionale di Fisica Nucleare, I-00044 Frascati, Italy*²⁰*University of Geneva, CH-1211 Geneva 4, Switzerland*²¹*Glasgow University, Glasgow G12 8QQ, United Kingdom*²²*Harvard University, Cambridge, Massachusetts 02138, USA*²³*Division of High Energy Physics, Department of Physics, University of Helsinki and Helsinki Institute of Physics, FIN-00014, Helsinki, Finland*

- ²⁴University of Illinois, Urbana, Illinois 61801, USA
²⁵The Johns Hopkins University, Baltimore, Maryland 21218, USA
²⁶Institut für Experimentelle Kernphysik, Universität Karlsruhe, 76128 Karlsruhe, Germany
²⁷Center for High Energy Physics: Kyungpook National University, Daegu 702-701, Korea; Seoul National University, Seoul 151-742, Korea; Sungkyunkwan University, Suwon 440-746, Korea; Korea Institute of Science and Technology Information, Daejeon, 305-806, Korea; Chonnam National University, Gwangju, 500-757, Korea
²⁸Ernest Orlando Lawrence Berkeley National Laboratory, Berkeley, California 94720, USA
²⁹University of Liverpool, Liverpool L69 7ZE, United Kingdom
³⁰University College London, London WC1E 6BT, United Kingdom
³¹Centro de Investigaciones Energeticas Medioambientales y Tecnologicas, E-28040 Madrid, Spain
³²Massachusetts Institute of Technology, Cambridge, Massachusetts 02139, USA
³³Institute of Particle Physics: McGill University, Montréal, Canada H3A 2T8; and University of Toronto, Toronto, Canada M5S 1A7
³⁴University of Michigan, Ann Arbor, Michigan 48109, USA
³⁵Michigan State University, East Lansing, Michigan 48824, USA
³⁶University of New Mexico, Albuquerque, New Mexico 87131, USA
³⁷Northwestern University, Evanston, Illinois 60208, USA
³⁸The Ohio State University, Columbus, Ohio 43210, USA
³⁹Okayama University, Okayama 700-8530, Japan
⁴⁰Osaka City University, Osaka 588, Japan
⁴¹University of Oxford, Oxford OX1 3RH, United Kingdom
⁴²University of Padova, Istituto Nazionale di Fisica Nucleare, Sezione di Padova-Trento, I-35131 Padova, Italy
⁴³LPNHE, Universite Pierre et Marie Curie/IN2P3-CNRS, UMR7585, Paris, F-75252 France
⁴⁴University of Pennsylvania, Philadelphia, Pennsylvania 19104, USA
⁴⁵Istituto Nazionale di Fisica Nucleare Pisa, Universities of Pisa, Siena and Scuola Normale Superiore, I-56127 Pisa, Italy
⁴⁶University of Pittsburgh, Pittsburgh, Pennsylvania 15260, USA
⁴⁷Purdue University, West Lafayette, Indiana 47907, USA
⁴⁸University of Rochester, Rochester, New York 14627, USA
⁴⁹The Rockefeller University, New York, New York 10021, USA
⁵⁰Istituto Nazionale di Fisica Nucleare, Sezione di Roma 1, University of Rome “La Sapienza,” I-00185 Roma, Italy
⁵¹Rutgers University, Piscataway, New Jersey 08855, USA
⁵²Texas A&M University, College Station, Texas 77843, USA
⁵³Istituto Nazionale di Fisica Nucleare, University of Trieste/Udine, Italy
⁵⁴University of Tsukuba, Tsukuba, Ibaraki 305, Japan
⁵⁵Tufts University, Medford, Massachusetts 02155, USA
⁵⁶Waseda University, Tokyo 169, Japan
⁵⁷Wayne State University, Detroit, Michigan 48201, USA
⁵⁸University of Wisconsin, Madison, Wisconsin 53706, USA
⁵⁹Yale University, New Haven, Connecticut 06520, USA

(Received 12 December 2007; published 14 March 2008)

We have performed a search for $B_s^0 \rightarrow \mu^+ \mu^-$ and $B^0 \rightarrow \mu^+ \mu^-$ decays in $p\bar{p}$ collisions at $\sqrt{s} = 1.96$ TeV using 2 fb^{-1} of integrated luminosity collected by the CDF II detector at the Fermilab Tevatron Collider. The observed number of B_s^0 and B^0 candidates is consistent with background expectations. The resulting upper limits on the branching fractions are $\mathcal{B}(B_s^0 \rightarrow \mu^+ \mu^-) < 5.8 \times 10^{-8}$ and $\mathcal{B}(B^0 \rightarrow \mu^+ \mu^-) < 1.8 \times 10^{-8}$ at 95% C.L.

DOI: [10.1103/PhysRevLett.100.101802](https://doi.org/10.1103/PhysRevLett.100.101802)

PACS numbers: 13.20.He, 12.15.Mm, 12.60.Jv

Processes involving flavor-changing neutral currents (FCNCs) provide excellent signatures with which to search for evidence of new physics since they have small branching fractions in the standard model (SM), while new physics contributions can provide a significant enhancement. The FCNC decays $B_s^0(B^0) \rightarrow \mu^+ \mu^-$ [1] occur in the SM only through higher order diagrams. The SM expectations for these branching fractions are $\mathcal{B}(B_s^0 \rightarrow \mu^+ \mu^-) = (3.42 \pm 0.54) \times 10^{-9}$ and $\mathcal{B}(B^0 \rightarrow \mu^+ \mu^-) = (1.00 \pm 0.14) \times 10^{-10}$ [2], which are 1 order of magnitude smaller

than current experimental sensitivity. Previous bounds, based on 1.3 fb^{-1} and 364 pb^{-1} are $\mathcal{B}(B_s^0 \rightarrow \mu^+ \mu^-) < 1.2 \times 10^{-7}$ and $\mathcal{B}(B^0 \rightarrow \mu^+ \mu^-) < 5.1 \times 10^{-8}$ at the 95% C.L., respectively [3,4].

Enhancements to $B_s^0(B^0) \rightarrow \mu^+ \mu^-$ occur in many new-physics models. In supersymmetry (SUSY) models, contributions from diagrams including supersymmetric particles can increase $\mathcal{B}(B_s^0(B^0) \rightarrow \mu^+ \mu^-)$ by several orders of magnitude at large $\tan\beta$, the ratio of vacuum expectation values of the Higgs doublets [5]. In the minimal super-

symmetric standard model (MSSM), the enhancement is proportional to $\tan^6\beta$. Global analyses including all existing experimental constraints suggest that the large $\tan\beta$ region is of interest [6–8]. In contrast, SUSY R -parity violating models [6] and nonminimal flavor violating models [9] can both enhance $B_s^0 \rightarrow \mu^+\mu^-$ and $B^0 \rightarrow \mu^+\mu^-$ separately even at low $\tan\beta$. In the absence of an observation, limits on $\mathcal{B}(B_s^0 \rightarrow \mu^+\mu^-)$ are complementary to those provided by other experimental measurements, and together would significantly constrain the allowed supersymmetric parameter space. For example, if the lightest neutralino in SUSY models is a cold dark matter (CDM) particle, $\mathcal{B}(B_s^0 \rightarrow \mu^+\mu^-)$ and constraints on the amount of CDM in the universe from cosmic microwave anisotropy measurements can be exploited in this way [6–8]. Then, for instance, in minimal supergravity (mSUGRA) models limits on $\mathcal{B}(B_s^0 \rightarrow \mu^+\mu^-)$ will correspond to bounds on superpartner particle masses that are beyond the sensitivity of the corresponding direct searches for those particles in colliding-beam experiments [6]. In general, the search for these rare decays is central to exploring a large class of new-physics models.

This measurement uses 2 fb^{-1} of integrated luminosity collected by the upgraded Collider Detector at Fermilab (CDF II) and supersedes our previous measurement using 364 pb^{-1} [4]. The sensitivity of the analysis is improved significantly by increasing the integrated luminosity of the event sample, using an enhanced muon selection, employing a neural network (NN) discriminant to separate signal from background, and performing the search in a two dimensional grid in dimuon mass and NN space.

A detailed description of the CDF II detector can be found in Ref. [10]. Charged particle tracking is provided by a silicon microstrip detector surrounded by an open-cell wire drift chamber immersed in a 1.4 T solenoidal magnetic field. This system provides precise vertex determination and momentum measurements for charged particles in a pseudorapidity range $|\eta| < 1.0$, where $\eta = -\ln(\tan\frac{\theta}{2})$ and θ is the angle of the track measured with respect to the proton beam direction. Additionally, the drift chamber measures the ionization per unit path length, dE/dx , for particle identification. Surrounding the tracking detectors are electromagnetic and hadronic sampling calorimeters arranged in a projective geometry. Drift chambers referred to as CMU and CMX are located behind the calorimeters to detect muons within $|\eta| < 0.6$ and $0.6 < |\eta| < 1.0$, respectively.

Events are recorded for subsequent analysis if they have either of two topologies that satisfy the requirements of the online trigger system: CMU-CMU, which includes events where both muon candidates are triggered using the central muon detectors, and CMU-CMX, which includes events where one of the muons is triggered in the central muon detector and one in the higher pseudorapidity region. The details of the trigger system and selection requirements can be found in Refs. [10,11].

In the offline analysis, the trigger selection is refined by applying a series of “baseline” requirements. We select two oppositely charged muon candidates within a dimuon invariant mass window of $4.669 < m_{\mu\mu} < 5.969 \text{ GeV}/c^2$ around the B_s^0 and B^0 masses. Backgrounds from hadrons misidentified as muons are suppressed by selecting muon candidates using a likelihood function. This function tests the consistency of electromagnetic and hadronic energy with that expected for a minimum ionizing particle and the differences between extrapolated track trajectories and muon system hits [12]. In addition, backgrounds from kaons that penetrate through the calorimeter to the muon system or decay in flight outside the drift chamber are further suppressed by a loose selection based on dE/dx [13]. The inputs to the muon likelihood and the dE/dx performance are calibrated using samples of $J/\psi \rightarrow \mu^+\mu^-$, $D^0 \rightarrow K^-\pi^+$ and $\Lambda \rightarrow p\pi^-$ decays. To reduce combinatorial backgrounds the muon candidates are required to have transverse momentum relative to the beam direction $p_T > 2.0(2.2) \text{ GeV}/c$ for CMU (CMX), and $|\vec{p}_T^{\mu\mu}| > 4 \text{ GeV}/c$, where $\vec{p}_T^{\mu\mu}$ is the transverse component of the sum of the muon momentum vectors. The remaining pairs of muon tracks are fit under the constraint that they come from the same three-dimensional (3D) space point. To achieve further separation of signal from background, we employ additional discriminating variables. As in our previous analysis [4] these include the measured proper decay time, λ ; the proper decay time divided by the estimated uncertainty, λ/σ_λ ; the 3D opening angle between vectors $\vec{p}^{\mu\mu}$ and the displacement vector between the primary vertex and the dimuon vertex, $\Delta\Theta$; and the B -candidate track isolation, I [14]. We require that $\lambda/\sigma_\lambda > 2$, $\Delta\Theta < 0.7 \text{ rad}$, and $I > 0.50$. There are 30 666 dimuon candidates that fulfill the above trigger and baseline reconstruction requirements. The baseline selection reduces combinatorial backgrounds by a factor of 300 while keeping approximately 50% of the signal events that are within the acceptance (geometric and kinematic requirements) of the trigger. Relative to the previous analysis, the application of the muon likelihood and dE/dx selection is approximately 97% efficient for the signal and reduces combinatorial backgrounds by 35% and constrains backgrounds from two-body hadronic B decays to a level that has negligible impact on the analysis. A sample of $B^+ \rightarrow J/\psi K^+$ events is collected to serve as a normalization mode using the same baseline requirements, but including a requirement of $p_T > 1 \text{ GeV}/c$ for the kaon candidate and constructing the $B^+ \rightarrow J/\psi K^+ \rightarrow \mu^+\mu^-$ vertex using only the muon candidate tracks.

For the final event selection we use the following discriminating variables: $m_{\mu\mu}$, λ , λ/σ_λ , $\Delta\Theta$, I , $|\vec{p}_T^{\mu\mu}|$, and the p_T of the lower momentum muon candidate. To enhance signal and background separation we construct a NN discriminant, ν_N , based on all the discriminating variables except $m_{\mu\mu}$, which is used to define signal and sideband

background regions. The NN is trained using background events sampled from the sideband regions and signal events generated with a simulation described below. The ν_N distributions of B_s^0 signal and sideband background events are shown in Fig. 1. Only part of the total number of background and simulated signal events are used in order to have unbiased samples to test the background discrimination and signal efficiency.

For the final selection, we define search regions of $5.310 < m_{\mu\mu} < 5.430$ GeV/ c^2 for the B_s^0 and $5.219 < m_{\mu\mu} < 5.339$ GeV/ c^2 for the B^0 around the mass values $m_{B_s^0} = 5.370$ GeV/ c^2 and $m_{B^0} = 5.279$ GeV/ c^2 [15], respectively. These regions correspond to approximately ± 2.5 times σ_m , the estimated two-track invariant mass resolution, where $\sigma_m \approx 24$ MeV/ c^2 . The sideband regions $4.669 < m_{\mu\mu} < 5.169$ GeV/ c^2 and $5.469 < m_{\mu\mu} < 5.969$ GeV/ c^2 are used to estimate the combinatorial backgrounds in the signal regions. Backgrounds from the two-body hadronic B_s^0 and B^0 decays, $B \rightarrow h^+ h^-$, where h^\pm are π^\pm or K^\pm , which peak in the B_s^0 and B^0 invariant mass signal region and do not occur in the sidebands, are estimated separately. The content of signal regions were not unveiled until all selection criteria were finalized. The final selection criteria were determined from an *a priori* optimization, which maximizes sensitivity of the expected limit. The kinematics of $B_s^0 \rightarrow \mu^+ \mu^-$ and $B^0 \rightarrow \mu^+ \mu^-$ decays are similar enough that the efficiencies are the same within statistical uncertainties and the same efficiencies and optimizations are used.

For measuring efficiencies, estimating backgrounds, and optimizing the analysis, samples of $B_s^0(B^0) \rightarrow \mu^+ \mu^-$, $B^+ \rightarrow J/\psi K^+$, and $B \rightarrow h^+ h^-$ are generated with the PYTHIA simulation program [16] and a CDF II detector simulation. The B -hadron p_T spectrum and the I distribution of the B hadrons are weighted to match distributions measured in samples of $B^+ \rightarrow J/\psi K^+$ and $B_s^0 \rightarrow J/\psi \phi$ events [10,12].

We use a relative normalization to determine the $B_s^0 \rightarrow \mu^+ \mu^-$ branching fraction:

$$\mathcal{B}(B_s^0 \rightarrow \mu^+ \mu^-) = \frac{N_s}{N_+} \frac{\alpha_+}{\alpha_s} \frac{\epsilon_+}{\epsilon_s} \frac{1}{\epsilon_N} \frac{f_u}{f_s} \mathcal{B}(B^+), \quad (1)$$

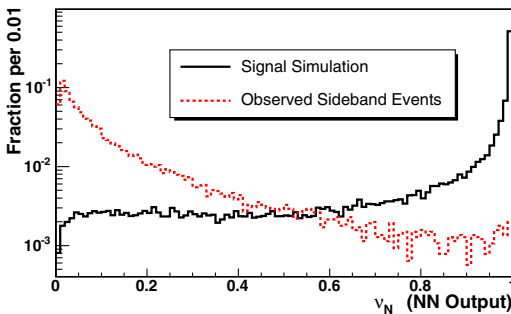


FIG. 1 (color online). Distributions of ν_N for simulated $B_s^0 \rightarrow \mu^+ \mu^-$ signal and observed sideband events.

where N_s is the number of $B_s^0 \rightarrow \mu^+ \mu^-$ candidate events. We observe $N_+ = 11\,387 \pm 164$ $B^+ \rightarrow J/\psi K^+$ candidates. This number has been corrected for background using sideband subtraction; the contribution of $B^+ \rightarrow J/\psi \pi^+$ events is negligible. We use $\mathcal{B}(B^+) = \mathcal{B}(B^+ \rightarrow J/\psi K^+ \rightarrow \mu^+ \mu^- K^+) = (5.94 \pm 0.21) \times 10^{-5}$ [15] and the ratio of B -hadron production fractions $f_u/f_s = 3.86 \pm 0.59$ [15]. The parameter α_s (α_+) is the acceptance of the trigger and ϵ_s (ϵ_+) is the efficiency of the reconstruction requirements for the signal (normalization) mode. The reconstruction efficiency includes trigger, track, muon, and baseline selection efficiencies. The NN efficiency, ϵ_N , only applies to the signal mode. The expression for $\mathcal{B}(B^0 \rightarrow \mu^+ \mu^-)$ is derived by replacing B_s^0 with B^0 and the fragmentation ratio with $f_u/f_d = 1$.

The ratios of acceptances α_+/α_s are 0.297 ± 0.020 and 0.191 ± 0.013 for the CMU-CMU and CMU-CMX trigger channels, respectively. These ratios are measured using simulated events, and the uncertainties include contributions from systematic variations of the modeling of the B -hadron p_T distributions, the longitudinal beam profile, and from the statistics of the simulated event samples. The ratio of reconstruction efficiencies is $\epsilon_+/\epsilon_s = 0.89 \pm 0.04$. Muon reconstruction efficiencies are estimated as a function of muon p_T using observed event samples of inclusive $J/\psi \rightarrow \mu^+ \mu^-$ decays. Systematic uncertainties in the efficiency ratio, ϵ_+/ϵ_s , largely cancel with the exception of the kaon efficiency from the B^+ decay. The uncertainty is dominated by kinematic differences between inclusive $J/\psi \rightarrow \mu^+ \mu^-$ and $B_s^0(B^0) \rightarrow \mu^+ \mu^-$ decays. The efficiency, ϵ_N , is estimated from the simulation. We assign a relative systematic uncertainty on ϵ_N of 6% based on comparisons of NN performance in simulated and observed $B^+ \rightarrow J/\psi K^+$ event samples and the statistical uncertainty on studies of the B_s^0 p_T and I distributions from observed $B_s^0 \rightarrow J/\psi \phi$ event samples. The NN provides approximately 25% better background rejection for the same signal efficiency compared to the previous analysis [4].

The expected background is obtained by summing contributions from the combinatorial continuum and from $B \rightarrow h^+ h^-$ decays. The contribution from other heavy-flavor decays is negligible. We estimate the combinatorial background by linearly extrapolating from the sideband region to the signal region. The $B \rightarrow h^+ h^-$ contributions are about a factor of 10 smaller than the combinatorial background and are estimated using efficiencies taken from the simulation, probabilities of misidentifying hadrons as muons measured in a $D^0 \rightarrow \pi K$ data sample, and normalizations derived from branching fractions from Refs. [13,15]. The two-body invariant mass distribution of the simulated $B \rightarrow h^+ h^-$ candidates is calculated from the momentum of the hadrons assuming the muon mass hypothesis. The background estimates are cross-checked using three independent control samples: $\mu^\pm \mu^\pm$

TABLE I. The total number of expected (Exp.) and observed (Obs.) background events for the B_s^0 (upper) and B^0 (lower) signal windows. ν_N bins: A (0.80–0.95), B (0.95–0.995), C (0.995–1.0) and five equal sized mass bins, (I–V), as described in the text.

B_s^0 ν_N	Mass bins				
	I	II	III	IV	V
A Exp.	10.3 ± 0.5	10.1 ± 0.4	9.9 ± 0.4	9.7 ± 0.4	9.5 ± 0.4
Obs.	11	9	10	9	5
B Exp.	3.7 ± 0.3	3.7 ± 0.3	3.6 ± 0.3	3.5 ± 0.3	3.5 ± 0.3
Obs.	4	3	6	6	2
C Exp.	0.7 ± 0.1	0.7 ± 0.1	0.7 ± 0.1	0.7 ± 0.1	0.7 ± 0.1
Obs.	0	1	1	0	1
B^0					
A Exp.	11.0 ± 0.6	10.8 ± 0.5	10.7 ± 0.5	10.5 ± 0.5	10.3 ± 0.5
Obs.	15	13	9	14	9
B Exp.	4.0 ± 0.3	3.9 ± 0.3	3.9 ± 0.3	3.8 ± 0.3	3.7 ± 0.3
Obs.	1	1	5	2	4
C Exp.	0.8 ± 0.1	0.8 ± 0.1	0.8 ± 0.1	0.8 ± 0.1	0.8 ± 0.1
Obs.	2	3	1	0	0

events, $\mu^+\mu^-$ events with $\lambda < 0$, and a misidentified muon-enhanced $\mu^+\mu^-$ sample in which we require one muon candidate to fail the muon quality requirements. We compare the predicted and observed number of events in these samples for a wide range of ν_N requirements and observe no significant discrepancies.

Using an *a priori* optimization procedure, we found that subdividing the signal region into several ν_N and mass bins to exploit the shape of the mass distribution and the higher signal to background ratios for the higher ν_N values improves the sensitivity by 15% relative to using a single bin. The signal region is divided into five equal mass bins of $24 \text{ MeV}/c^2$ and three ν_N bins delineated at 0.8, 0.95, 0.995, and 1.0. The backgrounds, efficiencies, and limits are calculated in each bin separately. Summing over the mass bins in each slice of ν_N , the corresponding ϵ_N 's are estimated to be 12%, 23%, and 44% and the expected SM yields of $B_s^0 \rightarrow \mu^+\mu^-$ events are 0.08 ± 0.03 , 0.15 ± 0.05 , and 0.30 ± 0.10 , respectively. The expected yield of $B^0 \rightarrow \mu^+\mu^-$ events is 10 times smaller. Using these optimized selection criteria, we compute an expected limit of $\mathcal{B}(B_s^0 \rightarrow \mu^+\mu^-) < 4.9 \times 10^{-8}$ at 95% C.L. The expected limit is a factor of 5 better than the expected limit of the previous analysis [4]. The limits are estimated from Eq. (1) using the confidence level method of Ref. [15] to extract the 95% C.L. upper bound on N_s ; the limit incorporates Gaussian uncertainties on the signal acceptance and efficiency as well as the background estimates. The number of observed events is compared with the total predicted background in Table I for each bin of mass and ν_N . The uncertainty on the background estimate is dominated by the statistical uncertainty of the sideband sample. The $\mu^+\mu^-$ invariant mass distributions for the three different ν_N ranges are shown in Fig. 2. The observed event rates are consistent with SM background expectations. We ex-

tract 95% (90%) C.L. limits of $\mathcal{B}(B_s^0 \rightarrow \mu^+\mu^-) < 5.8 \times 10^{-8}$ (4.7×10^{-8}) and $\mathcal{B}(B^0 \rightarrow \mu^+\mu^-) < 1.8 \times 10^{-8}$ (1.5×10^{-8}).

In mSUGRA, branching ratios as low as $\mathcal{B}(B_s^0 \rightarrow \mu^+\mu^-) = 5.8 \times 10^{-8}$ occur for common gaugino mass parameter, $m_{1/2}$, below $380 \text{ GeV}/c^2$ at $\tan\beta = 50$ in a CDM-allowed coannihilation region [17]. In this scenario we exclude gluino masses below $925 \text{ GeV}/c^2$.

This Letter reports a search for the rare FCNC decays $B_s^0 \rightarrow \mu^+\mu^-$ and $B^0 \rightarrow \mu^+\mu^-$ with 2 fb^{-1} integrated luminosity collected in $p\bar{p}$ collisions at $\sqrt{s} = 1.96 \text{ TeV}$ using the CDF II detector and employing improved analysis techniques. We observe no evidence for new physics

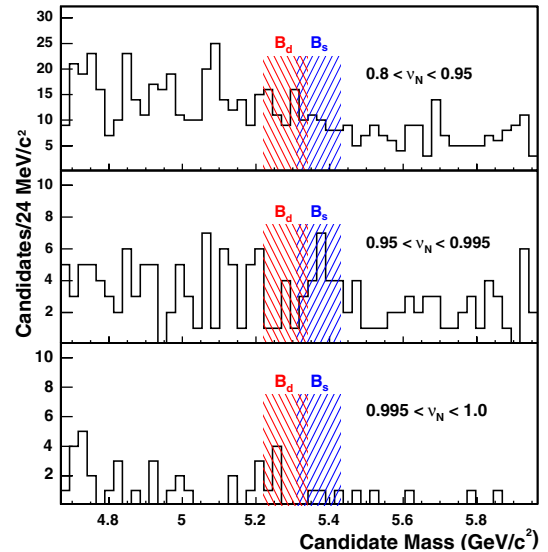


FIG. 2 (color online). The $\mu^+\mu^-$ invariant mass distribution for events satisfying all selection criteria for the final three ranges of ν_N .

and set limits that are the most stringent to date, improving the previous results [3,4] by a factor of 2 or more. These limits place further constraints on new-physics models [5–9], and complement direct searches for new physics. We expect the analysis sensitivity to continue to improve as we include larger data sets.

We thank the Fermilab staff and the technical staffs of the participating institutions for their vital contributions. This work was supported by the U.S. Department of Energy and National Science Foundation; the Italian Istituto Nazionale di Fisica Nucleare; the Ministry of Education, Culture, Sports, Science and Technology of Japan; the Natural Sciences and Engineering Research Council of Canada; the National Science Council of the Republic of China; the Swiss National Science Foundation; the A.P. Sloan Foundation; the Bundesministerium für Bildung und Forschung, Germany; the Korean Science and Engineering Foundation and the Korean Research Foundation; the Science and Technology Facilities Council and the Royal Society, UK; the Institut National de Physique Nucleaire et Physique des Particules/CNRS; the Russian Foundation for Basic Research; the Comisión Interministerial de Ciencia y Tecnología, Spain; the European Community’s Human Potential Programme; the Slovak R&D Agency; and the Academy of Finland.

^aVisitor from: University of Athens, 15784 Athens, Greece.

^bVisitor from: Chinese Academy of Sciences, Beijing 100864, China.

^cVisitor from: University of Bristol, Bristol BS8 1TL, United Kingdom.

^dVisitor from: University Libre de Bruxelles, B-1050 Brussels, Belgium.

^eVisitor from: University of California Irvine, Irvine, CA 92697, USA.

^fVisitor from: University of California Santa Cruz, Santa Cruz, CA 95064, USA.

^gVisitor from: Cornell University, Ithaca, NY 14853, USA.

^hVisitor from: University of Cyprus, Nicosia CY-1678, Cyprus.

ⁱVisitor from: University College Dublin, Dublin 4, Ireland.

^jVisitor from: University of Edinburgh, Edinburgh EH9 3JZ, United Kingdom.

^kVisitor from: University of Heidelberg, D-69120 Heidelberg, Germany.

^lVisitor from: Universidad Iberoamericana, Mexico D.F., Mexico.

^mVisitor from: University of Manchester, Manchester M13 9PL, United Kingdom.

ⁿVisitor from: Nagasaki Institute of Applied Science, Nagasaki, Japan.

^oVisitor from: University de Oviedo, E-33007 Oviedo, Spain.

^pVisitor from: Queen Mary, University of London, London, E1 4NS, United Kingdom.

^qVisitor from: Texas Tech University, Lubbock, TX 79409, USA.

^rIFIC (CSIC-Universitat de Valencia), 46071 Valencia, Spain.

- [1] Throughout this Letter inclusion of charge conjugate reactions are implied.
- [2] G. Buchalla and A.J. Buras, Nucl. Phys. **B400**, 225 (1993); A.J. Buras, Phys. Lett. B **566**, 115 (2003).
- [3] V. Abazov *et al.* (D0 Collaboration), Phys. Rev. D **76**, 092001 (2007).
- [4] D. Acosta *et al.* (CDF Collaboration), Phys. Rev. Lett. **95**, 221805 (2005).
- [5] S.R. Choudhury and N. Gaur, Phys. Lett. B **451**, 86 (1999); K.S. Babu and C. Kolda, Phys. Rev. Lett. **84**, 228 (2000).
- [6] R. Arnowitt *et al.*, Phys. Lett. B **538**, 121 (2002).
- [7] S. Baek *et al.*, J. High Energy Phys. **06** (2005) 017.
- [8] R. Ruiz de Austri *et al.*, J. High Energy Phys. **05** (2006) 002; J. Ellis *et al.*, J. High Energy Phys. **05** (2006) 063.
- [9] P.H. Chankowski and J. Rosiek, Acta Phys. Polon. **33**, 2329 (2002).
- [10] D. Acosta *et al.* (CDF Collaboration), Phys. Rev. D **71**, 032001 (2005).
- [11] D. Acosta *et al.* (CDF Collaboration), Phys. Rev. Lett. **93**, 032001 (2004).
- [12] A. Abulencia *et al.* (CDF Collaboration), Phys. Rev. Lett. **97**, 242003 (2006).
- [13] A. Abulencia *et al.* (CDF Collaboration), Phys. Rev. Lett. **97**, 211802 (2006).
- [14] $I = |\vec{p}_T^{\mu\mu}| / (\sum_i p_T^i + |\vec{p}_T^{\mu\mu}|)$; the sum is over all tracks with $\sqrt{\Delta\eta^2 + \Delta\phi^2} \leq 1$; $\Delta\phi$ and $\Delta\eta$ are the azimuthal angle and pseudorapidity of track i with respect to $\vec{p}^{\mu\mu}$.
- [15] W.-M. Yao *et al.*, J. Phys. G **33**, 1 (2006).
- [16] T. Sjöstrand *et al.*, Comput. Phys. Commun. **135**, 238 (2001).
- [17] In the mSUGRA model, we assume a common trilinear parameter $A_0 = 0$ and a positive Higgsino mixing parameter. In the coannihilation region, the difference of the neutralino and stau masses is characterized to be less than $20 \text{ GeV}/c^2$. See Ref. [6] for details.